Hindawi
Shock and Vibration
Volume 2020, Article ID 8888445, 10 pages
https://doi.org/10.1155/2020/8888445

Research Article

Wave Attenuation and Dispersion in a 6 mm Diameter Viscoelastic Split Hopkinson Pressure Bar and Its Correction Method

Haotian Zhang,[1] **Linjian Ma**,[1] **Zongmu Luo**,[1] **and Ning Zhang**[2]

[1]*State Key Laboratory of Disaster Prevention & Mitigation of Explosion & Impact, Army Engineering University of PLA, Nanjing 210007, China*
[2]*School of Science, Nanjing University of Science and Technology, Nanjing 210094, China*

Correspondence should be addressed to Linjian Ma; patton.4400@163.com

Received 28 June 2020; Revised 21 October 2020; Accepted 2 November 2020; Published 16 November 2020

Academic Editor: Marcello Vanali

The propagation characteristics of viscoelastic waves have been investigated with a 6 mm diameter split Hopkinson pressure bar (SHPB) made of polymethyl methacrylate (PMMA). The strain signals in SHPB tests were improved by the pulse shaping technique. Based on the experimentally determined propagation coefficients, the amplitude attenuation and wave dispersion induced by viscoelastic effects at different impact velocities were quantitatively analyzed. The results indicate that the high-frequency harmonics attenuate faster in a higher phase velocity. With an increase in the impact velocity, the amplitude attenuation of the viscoelastic wave changes slightly during propagation, while the waveform dispersion gradually intensifies. A feasible method by waveform prediction was proposed to verify the validity and applicability of the propagation coefficient. The results indicate that the strain obtained from the small diameter viscoelastic SHPB can be effectively modified by utilizing the propagation coefficient. Furthermore, it is preferred to adopt the propagation coefficient obtained at low impact velocity for correction when the impact velocity varies. Moreover, the PMMA-steel bar impact test was performed to further illustrate the accuracy of the propagation coefficient and the effectiveness of the correction method.

1. Introduction

It is well known that the split Hopkinson pressure bar (SHPB) is a widely utilized technique for exploring the dynamic mechanical behavior of materials [1–3]. Hundreds of literatures related to SHPB were published per year worldwide, mainly focusing on the characteristics of materials at high strain rates [4–6]. Particularly, numerical simulation provides the possibility to reveal the important micromechanism of wave propagation, specimen failure, and the strain rate effect in the SHPB test. Among the studies based on SHPB, obtaining appropriate stress wave signals is the key to get objective test results. Employing a proper pulse shaper is one of the effective methods to improve the incident waveform, which helps to achieve the dynamic equilibrium state and to meet the condition of constant strain rate in the test specimen [7, 8]. Alternatively, utilizing a special shape striker with a matched length to impact the incident bar is another approach to produce suitable compressive stress waves [8, 9]. The induced incident stress waves with enough long duration are necessary to guarantee the validity of SHPB experiments [10]. Moreover, the physical parameters, such as size and friction, of the compression bar and the specimen have a great influence on the test validity. Li et al. [11] reported that the strain rate effects on the strength of rock are related to radial confinement induced by axial strain acceleration, small aspect ratio, and friction constrains. They also indicated that the radial constraint effect can be reduced by replacing solid specimens with tubular specimens or by smaller specimen. Hao et al. [12] proposed empirical relations to eliminate the impacts of the lateral inertia confinement, so as to better explore the strain rate effects. Zhu et al. [13] introduced three methods to study the frictional effect between the rock sample and bars. They analyzed the effects of static axial pressure and lateral pressure and then determined the dynamic behavior of rocks under in situ stresses.

Although a great deal of laboratory experiments and numerical simulations has been conducted, there is no uniform standard for SHPB design. For different research purposes, scholars made efforts to modify the SHPB devices and optimize the wave signals to achieve more precise results. In the traditional SHPB experiments, the bars are commonly made of metal, and its wave impedance matches that of the specimen tested. Recently, with the continuous development of materials science, a large number of new materials have emerged [14–21]. Among them, polyurea, rubber, and foam materials have received increasing attention in packaging, transportation, military protection, and other fields, and their dynamic characteristics under impact loading have been well studied. However, compared with metallic materials, these materials have lower wave impedance. According to the propagation theory of stress waves, it is difficult to use the traditional steel or aluminum pressure bars for material testing mainly for two reasons [22]. First, the transmitted wave is too weak, resulting in a low signal-to-noise ratio. Second, the difference between the reflected wave and the incident wave is not enough to reflect the stress at the incident end, leading to errors in the result.

To solve the abovementioned problems, it is necessary to improve the SHPB technology by replacing the conventional metal bar with low-wave impedance bar. Nevertheless, the viscoelastic effect of the low-wave impedance materials (such as PMMA and nylon) cannot be neglected. As the wave propagates between the measuring point of the strain gauge and the end of bar, amplitude attenuation and waveform dispersion occur. In this case, the calculation method in the conventional SHPB test is no longer applicable and the difficulty and complexity of data processing increase. Based on the Zhu-Wang-Tang viscoelastic constitutive model, Wang et al. [23] studied the characteristic of viscoelastic wave propagation under impact load by means of numerical simulation. Zhao et al. [24, 25] extended the Pochhammer-Chree wave propagation model suitable for the elastic cylindrical rod to the linear viscoelastic cylindrical rod, so as to improve the measurement accuracy. However, the Pochhammer-Chree method needs to specify the constitutive model and corresponding material parameters of viscoelastic bar in advance. In contrast, the method proposed by Bacon [26] may conveniently obtain the propagation coefficient through experiments and then determine the attenuation and dispersion of waves in the viscoelastic bar. Liu et al. [27] studied the influence of the inertial effect adopting Bacon's theory and experimental methods. Cheng et al. [28] proposed a method for viscoelastic wave correction based on spectral analysis, and the feasibility of the method was demonstrated by simulation results. They also pointed out that the problem still arises from the effect of the rate-dependent property of viscoelastic material in the SHPB test.

Compared with previous studies, the influence of the transverse inertia effect could be ignored to a greater extent in the case of smaller-diameter viscoelastic bars [29, 30]. Besides, higher strain rates are convenient to be obtained utilizing small diameter SHPB. It is beneficial for studying the dynamic mechanical properties of materials, especially the low-impedance materials (such as rubbers [17], polymers [18, 19], and foams [20]). Therefore, it is of great importance to estimate the rate effect on wave propagation characteristic in a small diameter viscoelastic pressure bar and explore the specific method for correcting the test result. In this paper, a 6 mm diameter SHPB made of PMMA has been used to investigate the propagation law of viscoelastic stress waves. By improving the striker and using pulse shaping technology, the desired incident signal and reflected signal were obtained. The propagation coefficients at different impact velocities were experimentally determined. The rate effect on wave propagation characteristics in the viscoelastic bar was analyzed via the changes in attenuation coefficient and phase velocity. Finally, the accuracy of evaluated results of the propagation coefficients and the effectiveness of the correction method were verified by performing waveform prediction and PMMA-steel bar impact experiment.

2. Theory of One-Dimensional Linear Elastic Wave Propagation

Under the assumption of one-dimensional stress wave, the motion of a linear viscoelastic pressure bar (as shown in Figure 1) in the Fourier domain is governed by [26]

$$\frac{\partial^2}{\partial x^2}\widetilde{\sigma}(x,\omega) = -\rho\omega^2\widetilde{\varepsilon}(x,\omega), \tag{1}$$

where $\widetilde{\sigma}(x,\omega)$ and $\widetilde{\varepsilon}(x,\omega)$ are the Fourier forms of the stress and strain, ρ is the initial density, and $\omega = 2\pi f$ is the angular frequency. Under linear viscoelastic condition, the Fourier expression of material constitutive relation is

$$\widetilde{\sigma}(x,\omega) = E^*(\omega)\widetilde{\varepsilon}(x,\omega), \tag{2}$$

where $E^*(\omega)$ is Young's modulus in the complex form. To reflect the constitutive attenuation and dispersion caused by the viscoelastic effect, the propagation coefficient, $\gamma(\omega)$, is defined as $\gamma^2 = (-\rho\omega^2/E^*)$, and the general solution of equation (1) can be obtained as

$$\widetilde{\varepsilon}(x,\omega) = \widetilde{P}(\omega)e^{-\gamma x} + \widetilde{N}(\omega)e^{\gamma x}, \tag{3}$$

$$\gamma(\omega) = \alpha(\omega) + ik(\omega), \tag{4}$$

where $\widetilde{P}(\omega)$ and $\widetilde{N}(\omega)$ are the Fourier strains caused by the right traveling wave propagating along $+x$ and the left traveling wave propagating along $-x$ at $x = 0$, respectively. The propagation coefficient is composed of the attenuation coefficient, $\alpha(\omega)$, corresponding to the real part and the wave number, $k(\omega)$, corresponding to the imaginary part, while $k(\omega) = \omega/c(\omega)$, and $c(\omega)$ is the phase velocity. Among them, the attenuation coefficient reflects the attenuation speed of the harmonic amplitude during the viscoelastic wave propagation process, and the phase velocity is the propagation velocity of harmonic. The difference in propagation velocity may cause the disparity in the distance of harmonic wave propagation, resulting in the change of waveform, i.e., wave dispersion. Therefore, the phase velocity characterizes the degree of wave dispersion.

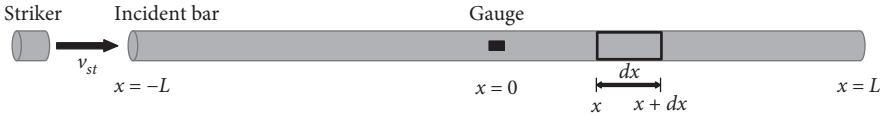

Figure 1: Schematic diagram of a linear viscoelastic bar under impact.

3. Experimental Equipment and Method

3.1. Experimental Equipment. The SHPB system employed in the experiment is composed of the pneumatic launcher, Hopkinson bars system, buffer device, and data acquisition system, as shown in Figure 2. The bars have the same cross-section with a diameter of 6 mm, and the incident bar and transmission bar are 600 mm and 500 mm in length, respectively. The density of PMMA is 1.19×10^3 kg/m^3. The specified strain gauge (model ZA120-02AA-Q30) with the base material of polyimide and the 2 mm length sensitive grid has been employed. The soft base material and the small dimension ensure that the strain gauge is able to stick tightly to the small diameter bar with the matched adhesive. The experimental operations of sticking strain gauges are performed under the magnifying lens with LED to ensure accuracy.

Before every impact test, nitrogen was filled into the gas gun through the gas cylinder, and the data collection system was adjusted to the state of "waiting to trigger." After turning on the solenoid valve, nitrogen was released from the gas storage chamber instantly, which drove the striker to collide with the incident bar. By adjusting the emission pressure in gas gun, different impact velocities can be obtained, which were measured by the laser velocimeter. The incident and reflected signals on the incident bar and transmitted signal on the transmission bar can be measured, respectively, through the strain gauges. The energy carried by the pulse was eventually dissipated by the buffer device.

3.2. Procedure of Determining the Propagation Coefficient. The experimental evaluation method for the propagation coefficient proposed by Bacon [26] has been used in this paper. During the experimental determination of the propagation coefficient, the incident bar and the transmission bar are placed in a noncontact state. To maximize the separation between the incident pulse and the reflected pulse on the incident bar, the strain gauges are attached on the middle of the incident bar, as shown in Figure 1. After the collision between the striker and the incident bar, the incident pulse starts from the collision end ($x = -L$) and reflects at the free end ($x = L$). The incident signal and the reflected signal monitored by the strain gauges are Fourier transformed to $\widetilde{\varepsilon}_i(\omega)$ and $\widetilde{\varepsilon}_r(\omega)$. Since the strain at the free end ($x = L$) is zero, it can be obtained by equation (3) that

$$\widetilde{\varepsilon}_L(x, \omega) = \widetilde{\varepsilon}_i(\omega) e^{-\gamma L} + \widetilde{\varepsilon}_r(\omega) e^{\gamma L} = 0, \tag{5}$$

and the expression for $\gamma(\omega)$ is

$$\gamma(\omega) = \frac{\ln\left(-\widetilde{\varepsilon}_r / \widetilde{\varepsilon}_i\right)}{-2L}. \tag{6}$$

The propagation coefficients can be obtained from the incident and reflected signals measured by the strain gauge, and the attenuation coefficient and phase velocity can be determined to study the propagation law of waves in the viscoelastic bar.

As is well known, the dynamic properties of viscoelastic materials are strain rate dependent. The dynamic stress-stain relationship of PMMA bar changes at different impact velocities, and the propagation coefficient varies accordingly. Therefore, it is necessary to study the influence of the impact velocity on the propagation coefficient. The impact velocity here is represented by the velocity of the striker as measured by the velocimeter. In this experiment, six levels of emission pressures between 350 kPa and 700 kPa were set to achieve the corresponding impact velocities between 5.10 m/s and 19.10 m/s. The viscoelastic effect may cause a great degree of time delay of incident waves [31]. To avoid the tail of the incident wave being superimposed with the reflected wave, the length of the striker is not suggested to exceed one quarter of that of the incident bar. Therefore, a PMMA striker with a length of 100 mm was used in the SHPB preexperiment. The signal on the incident bar and the relationship between amplitude and frequency are shown in Figure 3.

The result in Figure 3(a) shows that even when the length of the striker is one-sixth of the length of the incident bar, the incident wave and reflected wave cannot be effectively separated, which is different from the conclusion of Zhao et al. [31]. This may be due to the different properties or different processing processes of viscoelastic materials. As a result, the viscoelastic effect was more obvious in this experiment, causing a delay in pulse width. Therefore, the length of the striker was shortened to 15 mm as an improvement to ameliorate the experimental results. In addition, it was found that the harmonic amplitude fluctuates significantly between 30 kHz and 60 kHz in Figure 3(b), which brought difficulties to the Fourier transform in data processing. For this kind of high-frequency oscillation phenomenon, Guo [32] utilized the FFT filtering method to effectively obtain the dominant low-frequency harmonic frequency range. The method only ignored high-frequency waves in numerical calculations, but did not take into account the effect of high-frequency waves during the actual loading experiments. In the present research, pulse shaping technology with rubber (0.5 mm in thickness and 2 mm in diameter) has been adopted on subsequent experiments for two reasons. First, considering that the pulse shaper is very important in the SHPB experiment, the analysis of the wave after shaping is closer to the actual needs. Second, the filtering effect of shapers is able to reduce the high-frequency oscillation to decrease the error generated in the fast Fourier transform.

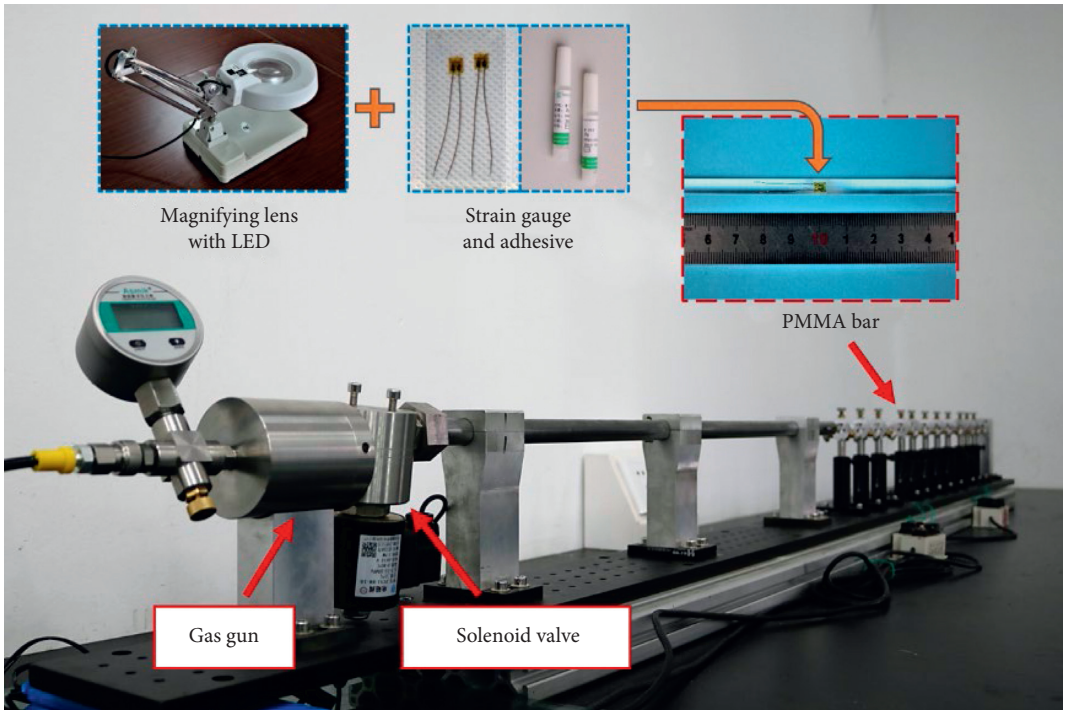

(a)

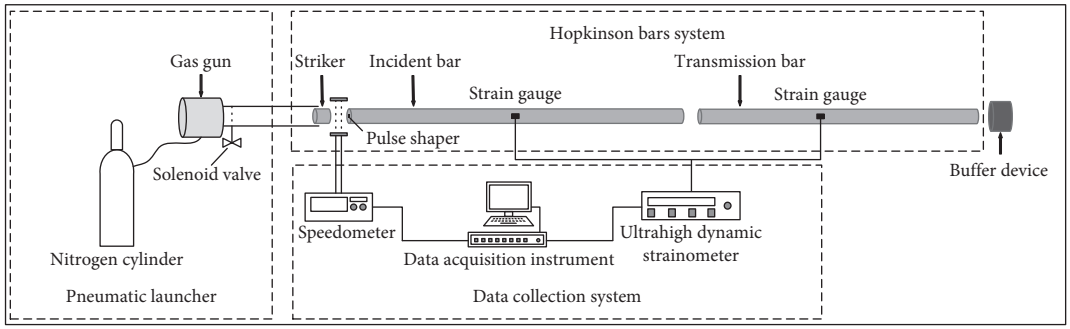

(b)

Figure 2: Φ6 mm SHPB experimental system. (a) Actual diagram. (b) Schematic diagram.

The improved signals on the incident bar at different impact velocities are shown in Figure 4, where the incident signals are not coupled with the reflected signals. The amplitude-frequency relationships of the incident waves are shown in Figure 5. By comparison, it can be seen that the plastic deformation of the pulse shaper blocks the high-frequency components in the incident wave. As a result, the harmonic components in the frequency range of 30 kHz–60 kHz reduce dramatically. After the improvement, the harmonic amplitude monotonically decays with an increase in the frequency and eventually drops to near zero before 40 kHz. Therefore, the dominant harmonic components below 40 kHz are the main concern in the following analysis of the propagation coefficient.

3.3. Verification of the Propagation Coefficient. Two means have been used to verify the effectiveness of the propagation coefficient. The feasibility of the correction method based on the propagation coefficient has also been illustrated. Based on the stress wave theory, the incident wave is completely reflected after it reaches the free end. Therefore, in the PMMA bar, the reflected wave should be the result of attenuation and dispersion after the incident wave propagates for a distance of $2L$. Combining equation (3), it can be expressed that

$$\widetilde{\varepsilon}_{r-\mathrm{pre}}(0,\omega) = -\widetilde{\varepsilon}_i(0,\omega)e^{-2\gamma_k L}, \tag{7}$$

where $\widetilde{\varepsilon}_i$ and $\widetilde{\varepsilon}_{r-\mathrm{pre}}$ are, respectively, the incident strain propagating along $+x$ and the predicted strain propagating along $-x$ in the frequency domain at $x=0$, and γ_k is the propagation coefficient obtained by experimental evaluation. According to equation (7), the reflected wave can be predicted by the propagation coefficient and the incident wave. By comparing the predicted waveform with the actually measured waveform, the effectiveness and applicability of the propagation coefficient can be initially verified. However, the calculation methods for the stress under

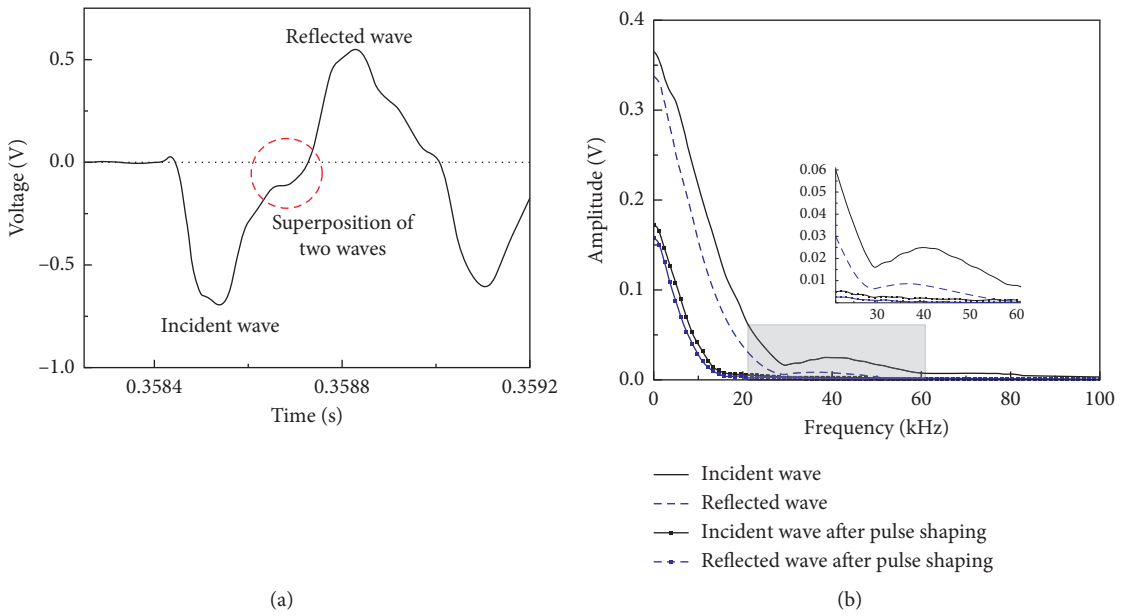

Figure 3: Results of preliminary experiment with an emission pressure of 350 kPa. (a) Signal on the incident bar. (b) Amplitude-frequency relationship.

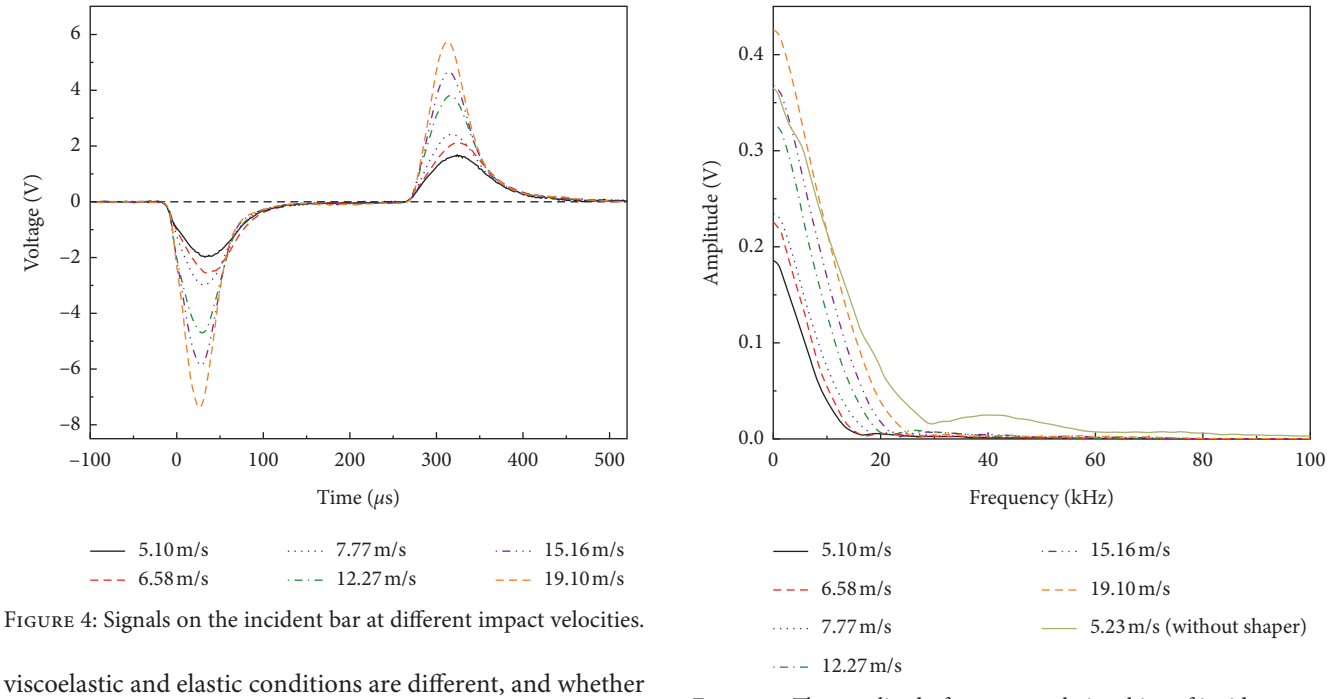

Figure 4: Signals on the incident bar at different impact velocities.

Figure 5: The amplitude-frequency relationships of incident wave at different impact velocities.

viscoelastic and elastic conditions are different, and whether the accurate stress value can be obtained needs to be further proved. Hence, the PMMA-steel bar impact test was carried out. By comparing the stresses measured by the two bars at the contact surface, a further verification of the correction method can be provided.

In the PMMA-steel bar impact test, the steel bar is used as the transmission bar to make alignment contact with the PMMA incident bar, so the stresses at the contact surface measured by the two bars should be equal after an impact test. According to the theory of Section 2 in this paper, the stress at the collision end of the incident bar can be obtained from

$$\tilde{\sigma}(L,\omega) = -\frac{\rho\omega^2}{\gamma^2}\left(\tilde{\varepsilon}_1(\omega)e^{-\gamma L} + \tilde{\varepsilon}_2(\omega)e^{\gamma L}\right), \tag{8}$$

where ε_1 and ε_2 are the incident and reflected signals measured by the strain gauge, and γ is the propagation coefficient evaluated by the determination experiment. The transmission bar is an elastic steel bar, so the reliable stress result at the collision end can be obtained by the calculation

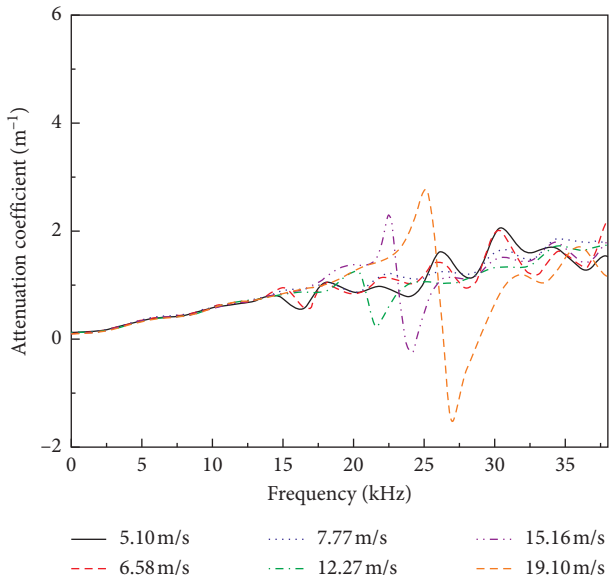

Figure 6: Relationship between attenuation coefficient and frequency at different impact velocities.

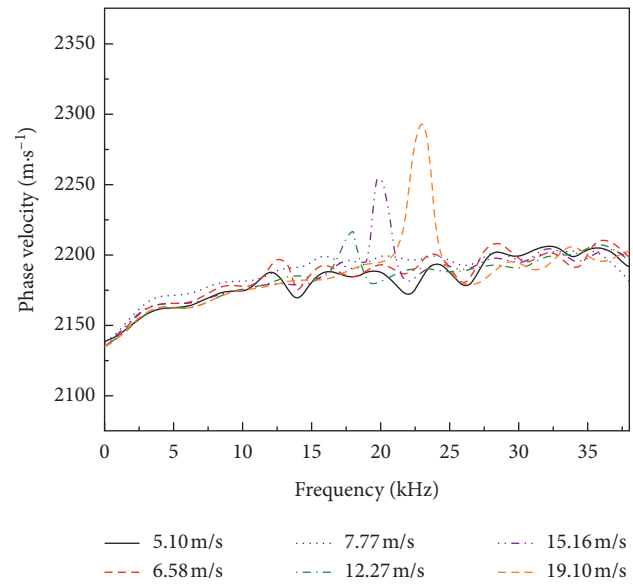

Figure 7: Relationship between phase velocity and frequency at different impact velocities.

method used in the conventional SHPB test [10]. By comparing the differences between the two results, the accuracy of the correction method based on the propagation coefficient can be evaluated and verified.

4. Results and Discussion

4.1. Attenuation and Dispersion in Wave Propagation. The signals on the incident bar in Figure 4 can be divided into incident waves and reflected waves by the threshold method. Then, the propagation coefficients are obtained by equation (6). The attenuation coefficients and phase velocities are obtained by equation (4). As shown in Figure 6, the attenuation coefficient increases with increasing frequency, indicating that the amplitude of harmonics at higher frequency attenuates faster. In the frequency range from 0 kHz to 14 kHz, the attenuation coefficients at different impact velocities are basically the same. As the frequency further increases, local convex peaks and concave valleys successively appear in the curves at different impact speeds, which are related to the numerical calculations involved in the fast Fourier transform [32]. Among them, the lower the impact velocity, the earlier the peak and valley appear. The higher the impact velocity, the higher the amplitude and the longer the duration. After peaks and valleys, the attenuation coefficient-frequency curves are again consistent.

The relationship between phase velocity and frequency at different impact velocities is shown in Figure 7, where phase velocities all start from 2138 m/s. It can be seen that the high-frequency harmonics have faster propagation speeds. The phase velocity rapidly increases within the frequency range of 0–3 kHz; then, it exhibits a decelerating growth trend. Starting from 11 kHz, local peaks appear in different curves. The causes and evolution laws are similar to the attenuation coefficient curve. Ultimately, the phase velocity all fluctuates at 2200 m/s before the harmonic frequency reaches 40 kHz. By comparing the curves under different impact velocities in the range of 0–25 kHz, it is found that the increase of impact velocity leads to the increase of phase velocities of harmonics. Hence, the difference of phase velocity between the harmonics is larger, which widens the propagation distance between the harmonics. Moreover, by observing the amplitude-frequency relationships between 0 kHz and 25 kHz in Figure 5, it is found that the harmonic amplitude of a certain frequency is higher under a higher impact velocity, which promotes the dispersion of the wave. Therefore, the dispersion of the wave in the propagation process is intensified under higher impact velocity.

4.2. Validity of the Propagation Coefficient

4.2.1. Waveform Prediction Based on the Propagation Coefficient. By comparing the predicted reflected wave with the measured reflected wave, the validity of the propagation coefficient can be verified. It should be noted that one cannot apply this method to the propagation coefficient and waveform obtained at the same impact velocity. Therefore, the propagation coefficient experimentally evaluated at impact velocity A and the incident waveform at impact velocity B was taken as a known condition to predict the reflection waveform at impact velocity B. Not only the validity of the propagation coefficient can be tested but also its applicability. The results of waveform prediction are shown in Figure 8.

As seen in Figure 8, the predicted waveforms agree well with the measured waveforms, which initially prove that the correction method based on the propagation coefficient is feasible. In other words, the propagation coefficient can reflect the attenuation and dispersion characteristics of the wave. By comparing the results of (a), (b), and (c), it is found that the result (a) is optimal. As the gap between velocity A and velocity B becomes larger, the predicted result gradually

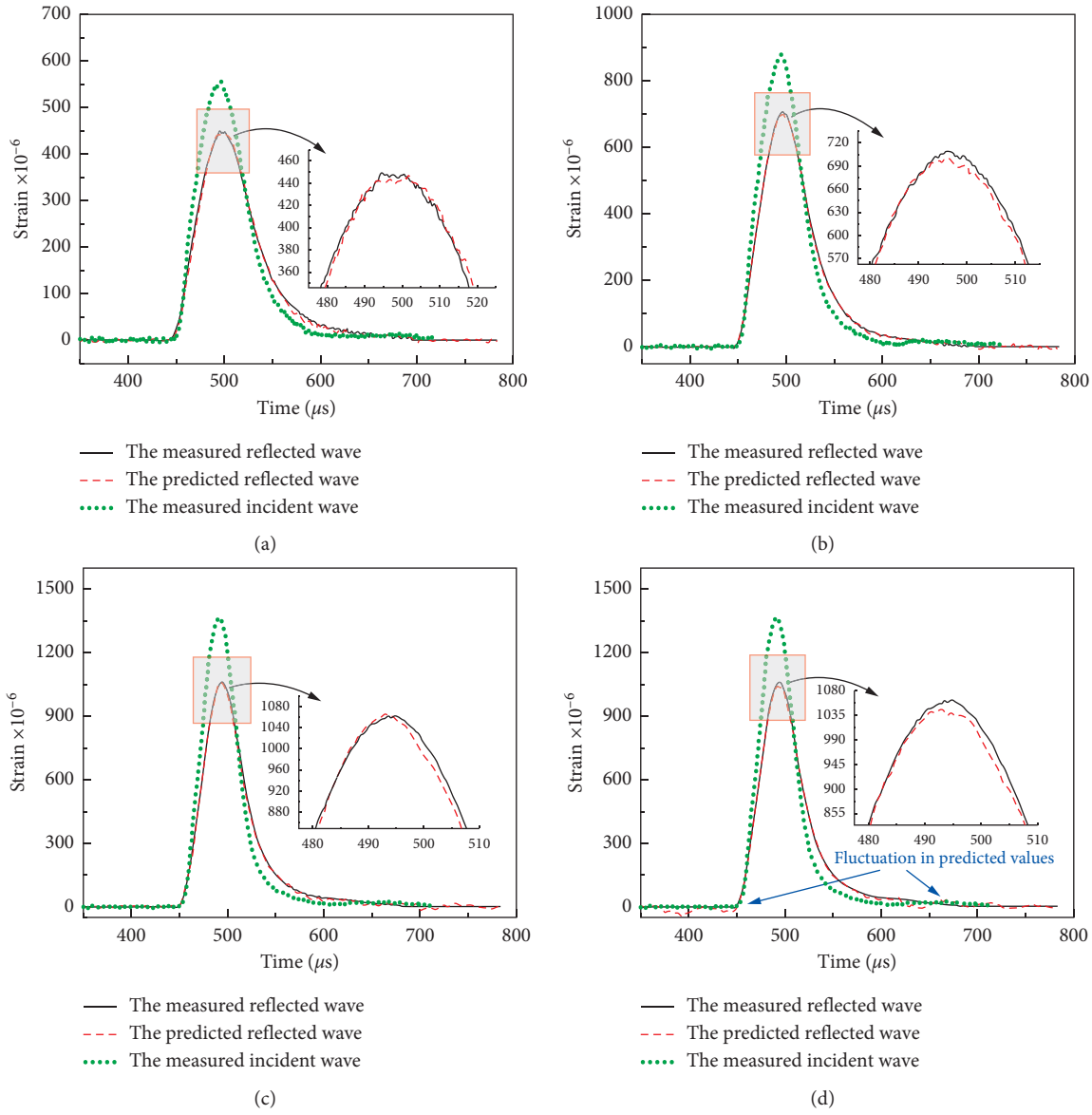

FIGURE 8: Waveform prediction results. (a) $A = 5.10$ m/s, $B = 7.77$ m/s. (b) $A = 5.10$ m/s, $B = 12.27$ m/s. (c) $A = 5.10$ m/s, $B = 19.10$ m/s. (d) $A = 12.27$ m/s, $B = 19.10$ m/s.

deviates from the measured results to a small extent. It can be found that when the impact velocity changes within a certain range, the same propagation coefficient can be used for correction.

In addition, the prediction results of (c) and (d) were compared. Although the gap between speed A and speed B in (d) was smaller, the prediction effect of (d) was not as good as (c). This paper believes that it is related to the peak-valley fluctuation in attenuation coefficient curves and phase velocity curves as shown in Figures 6 and 7. The peak-valley fluctuation represents the numerical oscillation of the real part and the imaginary part of the propagation coefficient. Such oscillations are more pronounced at high speeds, resulting in larger deviation in prediction. Therefore, when correcting the experimentally obtained waveform, it is recommended to use the propagation coefficient evaluated at a low speed.

4.2.2. Stress Calculation Based on the Propagation Coefficient. The collision test between the PMMA bar and steel bar was carried out to further verify the reliability of the propagation coefficient correction method. Young's modulus of steel is 210.1 GPa, the density is 7.8×10^3 kg/m^3, and the wave velocity is 5190 m/s. Figure 9 shows the typical strain signals in the incident bar and transmission bar at an impact velocity of 12.27 m/s. The incident strain and the reflected strain are both negative since the stress wave passes from a low-impedance material to a high-impedance material. In addition, the strain amplitude in transmission bar is smaller because

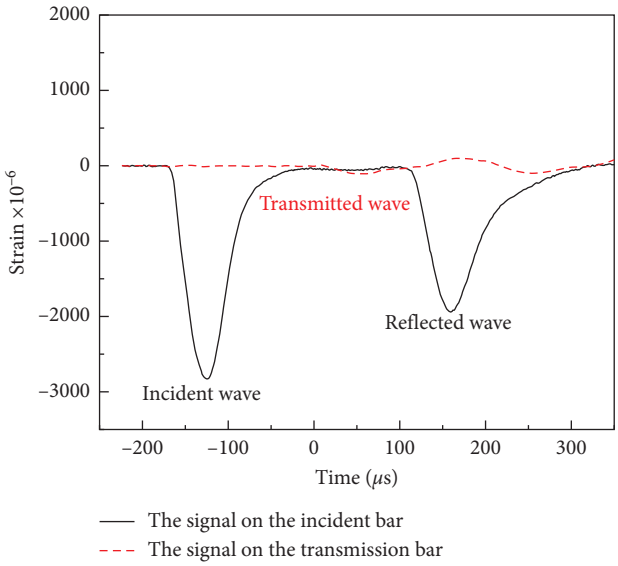

Figure 9: Results of the PMMA-steel bar impact test.

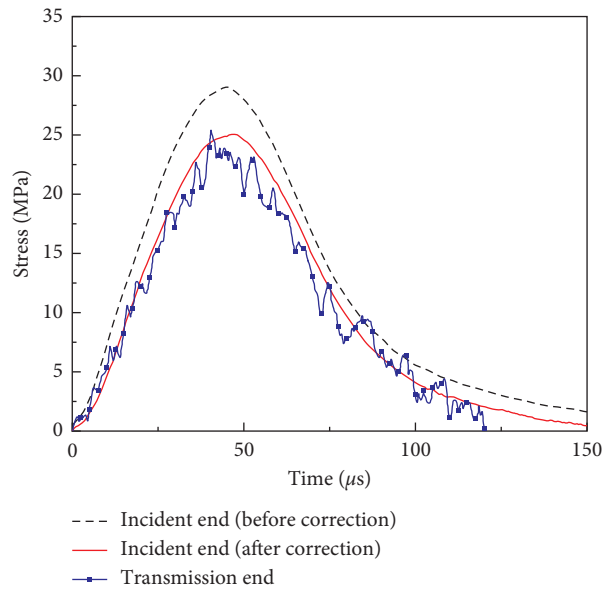

Figure 10: Comparison of stress calculated from elastic theory and viscoelastic theory.

Young's modulus of steel is much larger than that of PMMA subjected to the same contact force.

The stresses calculated by the elastic theory and the viscoelastic theory are plotted together in Figure 10, in which the dashed line represents the stress obtained from the signal on the incident bar by the elastic theory calculation method as

$$C_{\text{aver}} = \frac{2L}{\Delta t},$$
$$E_{\text{aver}} = \rho C_{\text{aver}}^2, \tag{9}$$
$$\sigma = E_{\text{aver}}(\varepsilon_i + \varepsilon_r),$$

where C_{aver} is the average wave velocity, L is the distance between the strain gauge and the end face, Δt is the time difference between the starting points of the incident and reflected waves, E_{aver} is the average Young's modulus, and ρ is the density of the PMMA bar. The average wave velocity obtained by the test was 2288.48 m/s, and the average Young's modulus was 6216.77 MPa. The solid line is the stress at the incident end calculated by equation (8), and the propagation coefficient used is the one evaluated by the experiment at an impact velocity of 5.10 m/s. Hence, the solid line represents the viscoelastic result based on the propagation coefficient. The line with data points is the result measured by the transmission bar made of steel. As is well known, the result obtained with traditional SHPB made of steel is reliable, which can be regarded as the actual result. In summary, the dashed line and the solid line represent the results before and after correction, respectively. It is evident that the result after correction is closer to the actual stress-time history curve. Hence, the validity of the correction method based on the propagation coefficient has been further verified.

5. Conclusions

A 6 mm diameter SHPB has been used to explore the viscoelastic wave propagation law. The effects of strain rate on wave attenuation and dispersion were researched. The validity and applicability of the correction method based on the propagation coefficient were assessed, which are helpful to the dynamic test on low-impedance materials. The main conclusions are drawn as follows:

(1) The wave propagation characteristics in viscoelastic bars are affected by impact velocity. At the same impact velocity, the harmonic attenuation coefficient and phase velocity gradually increase with increasing frequency, indicating that the high-frequency harmonic decay faster in a higher propagation speed. At different impact velocities, there is a little difference between the attenuation coefficient curves except for local peaks and valleys. The evolution laws of the phase velocity curves are roughly the same, whereas the differences in values are relatively large. Besides, the high-frequency harmonic wave with high amplitude induced by high impact velocity has an effect on the wave dispersion. Consequently, with an increase in the impact velocity, the attenuation of the amplitude during the viscoelastic wave propagation does not change much, while the wave dispersion intensifies.

(2) By comparing the predicted waveform with the measured waveform, it was found that the strain signal obtained in the small diameter SHPB test can be effectively corrected by utilizing the propagation coefficient. As the impact velocity changes, the same propagation coefficient can be used for correction. In addition, it is preferred to use the propagation coefficient evaluated at low impact velocity.

(3) The PMMA-steel bar impact test was conducted to further illustrate the validity of the correction method based on the propagation coefficient. The stress data measured by the steel bar is reliable, and it can be considered as the actual stress data to judge the validity of the result of the PMMA bar. By comparing the corrected data with uncorrected data, the accuracy of the propagation coefficient and the effectiveness of the correction method have been thoroughly verified.

Data Availability

The data used to support the findings of this study are available from the corresponding author upon request.

Conflicts of Interest

The authors declare that they have no conflicts of interest.

Acknowledgments

This work was financed and fully supported by the National Natural Science Foundation of China (Grant nos. 51774295 and 51808551), which is greatly appreciated by the authors. Useful suggestions given by Professor Mingyang Wang on the establishment of experimental equipment are also acknowledged.

References

[1] B. X. Hopkinson, "A method of measuring the pressure produced in the detonation of high, explosives or by the impact of bullets," *Philosophical Transactions of the Royal Society of London. Series A, Containing Papers of a Mathematical or Physical Character*, vol. 213, no. 497–508, pp. 437–456, 1914.

[2] R. M. Davies, "A critical study of the Hopkinson pressure bar," *Philosophical Transactions of the Royal Society of London. Series A, Mathematical and Physical Sciences*, vol. 240, no. 821, pp. 375–457, 1948.

[3] H. Kolsky, "An investigation of the mechanical properties of materials at very high rates of loading," *Proceedings of the Physical Society. Section B*, vol. 62, no. 11, p. 676, 1949.

[4] U. S. Lindholm, "Some experiments with the split Hopkinson pressure bar," *Journal of the Mechanics and Physics of Solids*, vol. 12, no. 5, pp. 317–335, 1964.

[5] J. E. Field, S. M. Walley, W. G. Proud, H. T. Goldrein, and C. R. Siviour, "Review of experimental techniques for high rate deformation and shock studies," *International Journal of Impact Engineering*, vol. 30, no. 7, pp. 725–775, 2004.

[6] L. Ma, Z. Li, J. Liu, L. Duan, and J. Wu, "Mechanical properties of coral concrete subjected to uniaxial dynamic compression," *Construction and Building Materials*, vol. 199, pp. 244–255, 2019.

[7] R. Naghdabadi, M. J. Ashrafi, and J. Arghavani, "Experimental and numerical investigation of pulse-shaped split Hopkinson pressure bar test," *Materials Science and Engineering: A*, vol. 539, pp. 285–293, 2012.

[8] Z. Y. Liao, J. B. Zhu, K. W. Xia, and C. A. Tang, "Determination of dynamic compressive and tensile behavior of rocks from numerical tests of split Hopkinson pressure and tension bars," *Rock Mechanics and Rock Engineering*, vol. 49, no. 10, pp. 3917–3934, 2016.

[9] X. Li, Y. Zou, and Z. Zhou, "Numerical simulation of the rock SHPB test with a special shape striker based on the discrete element method," *Rock Mechanics and Rock Engineering*, vol. 47, no. 5, pp. 1693–1709, 2014.

[10] W. C. Zhu, Y. Bai, X. B. Li, and L. L. Niu, "Numerical simulation on rock failure under combined static and dynamic loading during SHPB tests," *International Journal of Impact Engineering*, vol. 49, pp. 142–157, 2012.

[11] Q. M. Li, Y. B. Lu, and H. Meng, "Further investigation on the dynamic compressive strength enhancement of concrete-like materials based on split Hopkinson pressure bar tests. part II: numerical simulations," *International Journal of Impact Engineering*, vol. 36, no. 12, pp. 1335–1345, 2009.

[12] Y. Hao, H. Hao, and X. H. Zhang, "Numerical analysis of concrete material properties at high strain rate under direct tension," *International Journal of Impact Engineering*, vol. 39, no. 1, pp. 51–62, 2011.

[13] J. B. Zhu, Z. Y. Liao, and C. A. Tang, "Numerical SHPB tests of rocks under combined static and dynamic loading conditions with application to dynamic behavior of rocks under in situ stresses," *Rock Mechanics & Rock Engineering*, vol. 49, no. 10, pp. 1–12, 2016.

[14] L. M. Yang, V. P. W. Shim, and C. T. Lim, "A visco-hyperelastic approach to modelling the constitutive behaviour of rubber," *International Journal of Impact Engineering*, vol. 24, no. 6-7, pp. 545–560, 2000.

[15] W. Chen, F. Lu, and N. Winfree, "High-strain-rate compressive behavior of a rigid polyurethane foam with various densities," *Experimental Mechanics*, vol. 42, no. 1, pp. 65–73, 2002.

[16] J. McArthur, C. Salisbury, D. Cronin, M. Worswick, and K. Williams, "High strain rate characterization of shock absorbing materials for landmine protection concepts," *Shock and Vibration*, vol. 10, no. 3, pp. 179–186, 2003.

[17] B. Song and W. Chen, "One-dimensional dynamic compressive behavior of EPDM rubber," *Journal of Engineering Materials and Technology*, vol. 125, no. 3, pp. 294–301, 2003.

[18] B. Song, W. N. Chen, and X. Jiang, "Split Hopkinson pressure bar experiments on polymeric foams," *International Journal of Vehicle Design*, vol. 37, no. 2-3, pp. 185–198, 2005.

[19] J. Shim and D. Mohr, "Using split Hopkinson pressure bars to perform large strain compression tests on polyurea at low, intermediate and high strain rates," *International Journal of Impact Engineering*, vol. 36, no. 9, pp. 1116–1127, 2009.

[20] J. Liu, D. Saletti, S. Pattofatto, and H. Zhao, "Impact testing of polymeric foam using Hopkinson bars and digital image analysis," *Polymer Testing*, vol. 36, pp. 101–109, 2014.

[21] L. Ma, J. Wu, M. Wang, L. Dong, and H. Wei, "Dynamic compressive properties of dry and saturated coral rocks at high strain rates," *Engineering Geology*, vol. 272, Article ID 105615, 2020.

[22] H. Kolsky, *Stress Waves in Solids*, Vol. 1098, Courier Corporation, Chelmsford, MC, USA, 1963.

[23] L. Wang, K. Labibes, Z. Azari, and G. Pluvinage, "Generalization of split Hopkinson bar technique to use viscoelastic bars," *International Journal of Impact Engineering*, vol. 15, no. 5, pp. 669–686, 1994.

[24] H. Zhao and G. Gérard, "A three dimensional analytical solution of the longitudinal wave propagation in an infinite linear viscoelastic cylindrical bar. application to experimental techniques," *Journal of the Mechanics and Physics of Solids*, vol. 43, no. 8, pp. 1335–1348, 1995.

[25] H. Zhao, "Testing of polymeric foams at high and medium strain rates," *Polymer Testing*, vol. 16, no. 5, pp. 507–516, 1997.
[26] C. Bacon, "An experimental method for considering dispersion and attenuation in a viscoelastic Hopkinson bar," *Experimental Mechanics*, vol. 38, no. 4, pp. 242–249, 1998.
[27] X. M. Liu, X. S. Hu, and Z. Chen, "The wave propagation attenuation and dispersion in a viscoelastic Hopkinson pressure bar," *Chinese Journal of Solid Mechanics*, vol. 23, no. 1, pp. 81–86, 2002, in Chinese.
[28] Z. Q. Cheng, J. R. Crandall, and W. D. Pilkey, "Wave dispersion and attenuation in viscoelastic split Hopkinson pressure bar," *Shock and Vibration*, vol. 5, no. 5-6, pp. 307–315, 1998.
[29] J. W. S. B. Rayleigh, *The Theory of Sound*, Vol. 2, Macmillan, New York, NY, USA, 1896.
[30] P. S. Follansbee and C. Frantz, "Wave propagation in the split Hopkinson pressure bar," *Journal of Engineering Materials and Technology*, vol. 105, no. 1, pp. 61–66, 1983.
[31] H. Zhao, G. Gary, and J. R. Klepaczko, "On the use of a viscoelastic split Hopkinson pressure bar," *International Journal of Impact Engineering*, vol. 19, no. 4, pp. 319–330, 1997.
[32] L. L. Guo, *Computational Simulation and Experimental Research on the Wave Propagation in Viscoelastic Bar*, China Academy of Engineering Physics, Chengdu, China, 2005, in Chinese.